Journal of Materials Chemistry

Cite this: *J. Mater. Chem.*, 2012, **22**, 18646

www.rsc.org/materials

PAPER

Centrifugal electrospinning of highly aligned polymer nanofibers over a large area†

Dennis Edmondson,‡ Ashleigh Cooper,‡ Soumen Jana, David Wood and Miqin Zhang*

Received 15th June 2012, Accepted 20th July 2012
DOI: 10.1039/c2jm33877g

Well-ordered one-dimensional nanostructures are enabling important new applications in textiles, energy, environment and bioengineering owing to their unique and anisotropic properties. However, the production of highly aligned nanofibers in a large area remains a significant challenge. Here we report a powerful, yet economical approach that integrates the concepts of the parallel-electrode electrospinning with centrifugal dispersion to produce nanofibers with a high degree of alignment and uniformity at a large scale. We first demonstrated this approach with polyvinylidene fluoride to show how experimental parameters regulate fiber properties, and then with chitosan, a natural polymer, and polyethylene oxide, a synthetic polymer, to illustrate the versatility of the system. As a model application, we then demonstrated the significance of fiber alignment in improving the piezoelectric effect for voltage generation. The technique presented here may be used for mass production of aligned nanofibers of various polymers for a myriad of applications.

Introduction

Nanoscale fibers are widely used in textile, energy, environmental and bioengineering applications as they exhibit unique optical,[1] electrical,[2] mechanical,[3] and biological[4] properties that are not found in their bulk counterparts. Some of these applications require highly ordered, well-aligned fiber architectures in order to provide the required physical, mechanical, chemical or electrical anisotropy. For example, aligned polymer fibers of various compositions are able to regulate cell migration, proliferation, and differentiation, which is critical for tissue engineering.[5,6] Highly aligned polyfluorene-based nanofibers can increase charge-carrier mobility or enhance photoluminescence in the fiber alignment direction.[7] Composite electrolyte membranes with aligned polyimide-based fibers demonstrate greater proton-conduction for enhanced fuel cell efficiency.[8] Electrospinning has emerged as a simple, flexible, and versatile technique for creating many nanofiber-based materials.[9]

The production of aligned nanofibers by electrospinning is commonly achieved by use of specially designed fiber collectors, most notably, a fast rotating mandrel collector[10,11] or a parallel-electrode collector.[12] In a rotating collector configuration, the produced polymer fibers are deposited on and wrapped around a rotating mandrel.[10,11,13] The degree of fiber alignment largely depends on the mandrel rotational speed. In a parallel-electrode configuration, the insulating gap (mostly an air gap) between two parallel electrodes serves as the fiber collector, and charged fibers are aligned up across the gap by the electric field near the electrodes that points perpendicularly to the electrode edges;[14] the length of the aligned fibers is limited by the width of the insulating gap.[15] This configuration bears the advantage that the fibers can be easily removed from the collector, but the degree of fiber alignment decreases as the thickness of the fibrous mat increases due to the reduced electric field strength caused by the accumulated charge of the deposited nanofibers.[13,16] Alternative to collector modification, centrifugal dispersion of polymer solution has been recently explored to produce aligned fibers.[17,18] In this system configuration, a centrifugal force disperses a polymer–solvent solution through a capillary, which causes elongation and thinning of the solution jet, and the fiber is produced with no applied voltage.

Despite these exciting advancements, an electrospinning system that is suitable for large-scale production of nanofibrous structures while retaining a high degree of fiber alignment has yet to be demonstrated. Here, we present a hybrid electrospinning system capitalizing on the fiber alignment mechanisms of both the parallel-electrode method and centrifugal dispersion that can produce highly aligned polymer nanofibers at a large scale. We first demonstrate the capability of this system using polyvinylidene fluoride (PVDF) as a model polymer due to the favorable piezo-, pyro-, and ferro-electric properties that aligned PVDF fibers can provide for applications in actuators, transistors, textiles and composites.[19] We then further demonstrate the versatility of the system with two additional polymers, chitosan (a natural polymer) and polyethylene (a synthetic polymer), that

Department of Materials Science and Engineering, University of Washington, 302L Roberts Hall, Box 352120, Seattle, WA 98195, USA. E-mail: mzhang@u.washington.edu; Fax: +1 206-543-3100; Tel: +1 206-616-9356

† Electronic supplementary information (ESI) available. See DOI: 10.1039/c2jm33877g

‡ These authors contributed equally to this work.

have shown a wide range of applications in medicine, biotechnology and food industries.

Experimental

Centrifugal electrospinning system setup

The CE system includes a syringe-needle-spinneret positioned on a rotating hub driven by a variable speed electric motor (Amtek, Monrovia, CA). The spinneret is connected to an A30, 30 kV dc voltage power supply (Ultravolt, Ronkonkoma, NY) and centered in a non-conductive cylindrical housing with a diameter that can be varied from 2 to 4 feet. Eight aluminum plates (electrodes), each attached to a grounded, 0.5 inch diameter aluminum rod, are secured to the non-conducting housing, concentrically surrounding the central hub (Fig. 1).

Polymer solutions for electrospinning

Polyvinylidene fluoride tetrafluoroethylene and polyvinylidene fluoride (PVDF) (Arkema Corporation, King of Prussia, PA) were mixed at a weight ratio of 70/30. The polymer mixture was dissolved in dimethyl formamide (DMF)–acetone at a weight ratio of 60/40 to create final polymer concentrations between 20 and 27.5 wt%. To aid in the dissolution, the PVDF solution was refluxed at 80 °C for 30 min.

Centrifugal electrospinning setup characterization

A 20 wt% PVDF solution was electrospun using a 25 gauge needle (0.26 mm ID), at a voltage of 12 kV dc, and a spinneret–collector distance of 20 cm. As a control, a low pressure of 0.1 psi was applied to the syringe to drive the flow of polymer solution which was electrospun without spinneret rotation to illustrate static dispersion and parallel electrode deposition. The same solution was then electrospun with the spinneret rotated at 100, 200, 300 and 400 rpm. To determine the influence of the polymer concentration on the fiber diameter, the PVDF concentration was varied between 20 and 27.5 wt% in the DMF–acetone solution. From these tests, a rotational speed of 200 rpm was chosen as the spinneret speed.

Fiber characterization

Fibers were retrieved from the gaps of electrodes, sputter-coated with Au/Gd for 30 seconds at 18 mA, and imaged with a SEM (JOEL JSM 7000F) at an operating voltage of 5 kV. Fast Fourier transform (FFT) was performed using ImageJ (NIH, Bethesda, Maryland, USA) on a representative image to determine the fiber alignment. Specifically, an image was uploaded into ImageJ software and FFT analysis produced a pixel intensity image based on the frequency and direction of the fibers. The FFT images were normalized to a vertical axis with a baseline value of zero and radial pixel summing was performed using an oval prolife plug-in.[20] The FFT data were plotted over 180° as the FFT image is symmetric about the horizontal axis.

To demonstrate the piezoelectric functionality of PVDF fibers, fibers were electrospun from a 20 wt% PVDF in DMF–acetone solution containing 3 wt% tetrabutylammonium chloride (TBAC), which increases the solution conductivity to increase the electrospinnability and effectively increases the β-phase formation to contribute to the piezoelectric effect.[19] Samples were electrospun across a three-inch gap to form aligned fibers, and randomly oriented fibers were collected from the collector plate. Samples were also retrieved from a stationary dispersion condition (without spinneret rotation) across the same four-inch gap to illustrate a conventional parallel-electrode configuration. The sample dimensions were 0.74 mm^2 by 25 mm long. The fiber specimens were encased in PDMS, forming a cantilever beam with exposed fibrous ends. The specimens were tested according to the schematic in Fig. 6a. Electrodes were connected to the exposed fibers *via* conductive silver epoxy and connected to an Agilent 34420A NanoVolt meter that transmits voltage data to a computer running LabVIEW software *via* a custom vi program. The fiber specimen/PDMS samples were clamped to a support

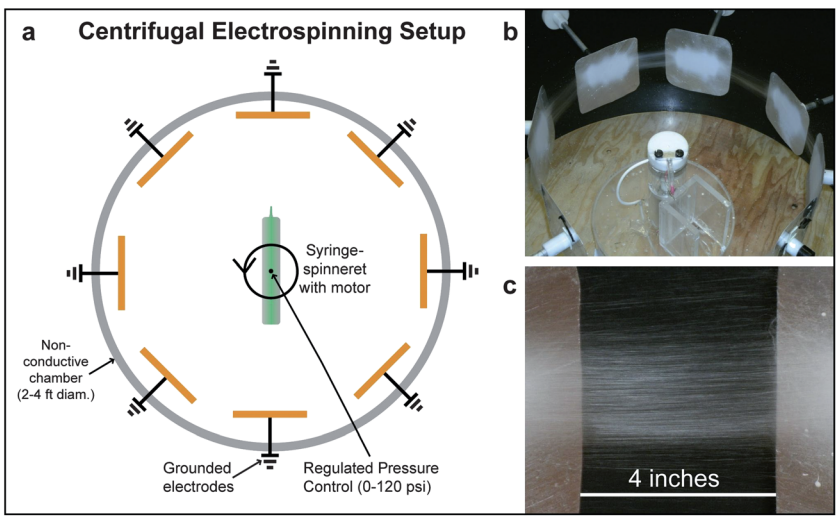

Fig. 1 Centrifugal electrospinning (CE) system for large-area production of aligned polymer nanofibers. (a) Schematic illustration of the system configuration. (b) Photograph of the CE system with deposited PVDF nanofibers. (c) Electrospun PVDF fibers deposited across a four-inch gap between two grounded electrodes.

mounted on a nanomechanical tester developed in our lab.[21] The entire testing system was kept in a quiescence state for 120 seconds before initiating beam deflection of the sample. The cantilever beam was deflected at 9.70 mm min^{-1} for 30 seconds. Three separate samples were tested and the results were averaged and normalized.

X-ray diffraction analysis was performed to determine the relative crystalline phases that contribute to the PVDF piezoelectric response. PVDF TBAC samples were prepared for using powder, films, and fibers in the form of random, stationary aligned (parallel-electrode) and centrifugally aligned (200 rpm) configurations. All samples were immobilized on a silicon substrate to reduce background noise. A Bruker D8 Discover XRD system with general area detector diffraction systems was used to probe the two theta range of 16–28°. Analysis was performed with Jade software and plotted with relative intensities for direct comparison of the diffraction peak locations.

Results and discussion

Centrifugal electrospinning system

The primary components of this centrifugal-electrode electrospinning (CE) system are a rotating hub hosting a spinneret (or, syringe-needle) and an array of grounded plate electrodes that circularly surround the rotating hub (Fig. 1a). The spinneret powered by a high-voltage power supply dispenses the polymer solution while the grounded electrodes introduce a fringe electrostatic field facilitating fiber alignment when charged fibers are deposited across the gaps (*i.e.*, collectors) between the neighboring electrodes (Fig. 1b). In addition to the alignment by the electrostatic force, the solution jet gains additional momentum towards the direction of fiber alignment upon exit from the spinneret due to the centrifugal force created by the rotating spinneret. As the leading tip of a fiber is deposited on an electrode, the fiber follows a continuous curvilinear path as the polymer solution is continuously dispersed from the rotating spinneret with the trailing end deposited on the neighboring electrode, enhancing the fiber alignment. The length of the aligned fibers is defined by the width of the gap, and typically, nanofibers of a few inches in length can be readily produced (Fig. 1c).

Clearly, as with any electrospinning systems, the formation and characteristics of nanofibers for each polymer solution (type and concentration) are strongly dependent on the system operating parameters, such as the net charge density (or supplied voltage), width of the electrode gap, and spinneret rotating speed (for our CE system). Here we have illustrated how these parameters affect the properties of electrospun nanofibers using PVDF as a model polymer system.

Spinneret rotating speed

In a conventional electrospinning process, polymer solution in the reservoir is electrostatically charged and when the applied electric field gradient overcomes the surface tension of the polymer solution, a Taylor cone forms at the tip and outside of the spinneret. The electrostatic force causes a solution jet to form at the tip of the Taylor cone and the solution jet elongates towards the collector, wherein the solvent evaporates, producing charged polymer fibers.[22] In our CE system, a radial force created by centrifugal dynamics helps stretch the polymer solution that exits the spinneret tip. If the rotation speed of the spinneret is zero, the CE system is analogous to a traditional parallel-electrode configuration.

To see how the centrifugal dispersion affects the properties (diameter, uniformity and alignment) of electrospun fibers, a series of experiments with sequentially increased rotational speeds were used to dispense a 20 wt% PVDF solution. As shown in Fig. 2a, with a stationary spinneret (*i.e.*, the rotating speed = 0), produced PVDF fibers were mostly aligned but misaligned fibers and a few beads were present. As the spinneret rotating speed was increased, the degree of fiber alignment increased. At the spinneret rotating speed of 200–300 rpm, no apparent misalignment was observed. Further increase in the rotating speed resulted in decreased fiber yield, and at a rotational speed of 400 rpm, no fibers could be collected, indicating that a too-high rotational speed would impede continuous fiber formation for the polymer solution used here.

FFT analysis was performed on the SEM images to determine the relative degree of fiber alignment based on the conversion of the image into frequency spacing (Fig. 2b). A dispersed, randomly oriented fiber sample exhibits a radially diffuse image in FFT analysis, while a highly aligned fiber sample exhibits a high intensity line normal to the fiber orientation. The FFT images were then analyzed with an oval-plot profile, wherein the radial intensity was summed and plotted with respect to the angle of acquisition. As shown in Fig. 2c, the fibers prepared at 200 rpm had the narrowest peak, with the smallest area underneath the curve, indicating that this rotational speed produced the highest degree of fiber alignment. Fibers produced from the stationary spinneret were least aligned.

In addition to the fiber alignment, the fiber morphology changed with the spinneret rotational speed. At zero or low (100 rpm) rotational speeds, a beads-on-a-string structure was observed. With stationary-spinneret dispersion, the high surface tension of the solution predominated the fiber formation, wherein the viscoelastic force in the solution resisted changes to the fiber jet shape, resulting in the beads-on-a-string structure.[23] With increasing spinneret rotational speed, the fiber uniformity increased and the number of beads in the fiber mat was reduced. At 200 rpm, no beads were observed, indicating that the centrifugal force effectively overcame the surface tension. At a higher speed of 300 rpm, the degree of fiber alignment remained high, but a few beads reappeared. At an even higher speed (400 rpm), only beads were produced (data not shown). The bead formation at these high rotational speeds was likely due to destabilization of the polymer solution by the increased centrifugal force, which might have prevented the formation of the Taylor cone and subsequent fiber formation. The destabilization occurs when the delivery rate of the solution to the spinneret tip was smaller than the rate at which the solution is removed by electrostatic and centrifugal forces, leading to non-continuous fiber formation.

Notably, a decrease in fiber diameter was observed with increasing spinneret rotating speed (Fig. 2d). The diameter of fibers produced from the stationary spinneret was 345 nm and decreased to 224 nm at a spinneret rotating speed of 300 rpm. The decrease in fiber diameter was attributed to the enhanced

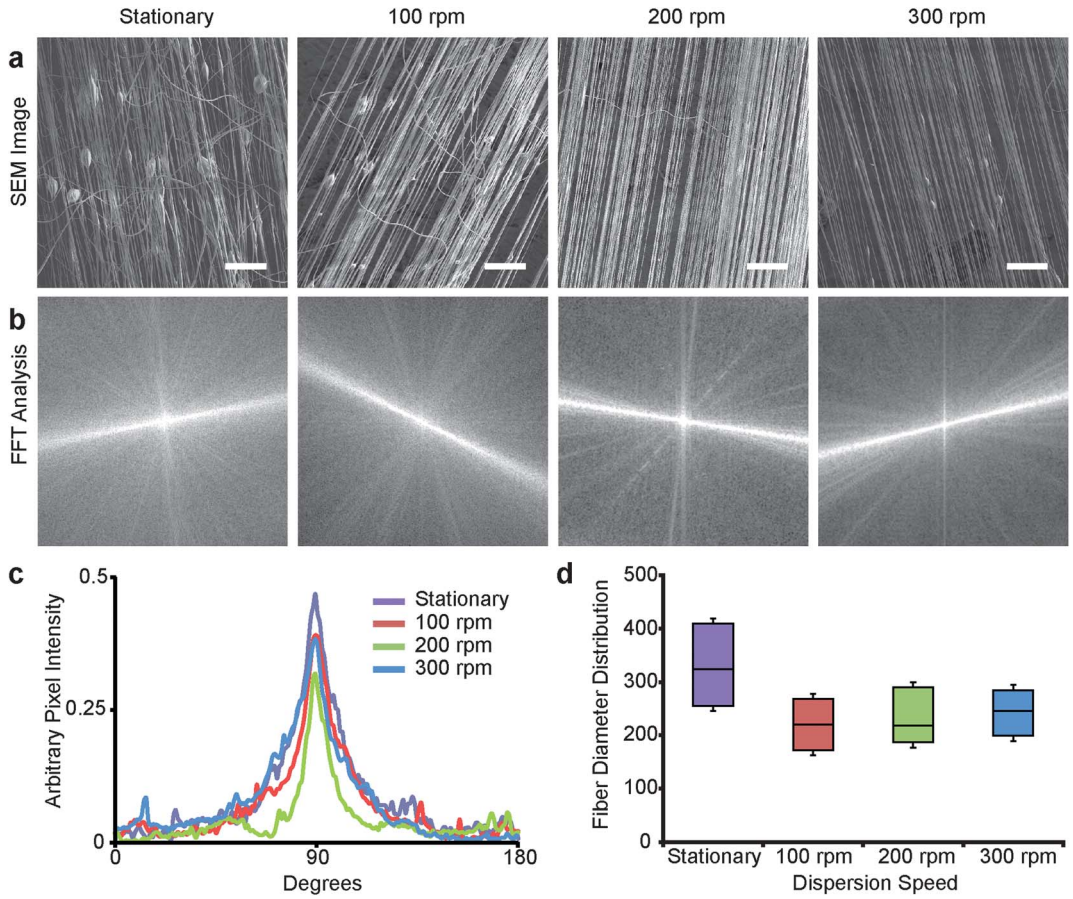

Fig. 2 PVDF fibers produced at various spinneret rotating speeds. (a) SEM images of PVDF nanofibers (scale bars = 20 μm) deposited across a four-inch gap from a 20 wt% polymer solution electrospun at 12 kV. (b) FFT analysis illustrating the degree of fiber alignment. (c) Arbitrary pixel intensity plotted from the radial summation of pixel intensity from the FFT analysis. (d) Fiber diameter distribution with the median diameter represented by the horizontal line shown in the middle of the bar. The error bars indicate the largest and smallest fiber diameters measured from a dataset of 50 fibers.

elongation (and thinning) of the solution jet by the increased centrifugal force at the fixed solution-feeding rate. Based on these results, we concluded that a spinneret speed of 200 rpm produces the most aligned, uniform and smallest diameter fibers from a 20 wt% PVDF solution.

Electrode gap width

The parallel-electrode gap width has a significant impact on the fiber alignment and dictates the ability of the CE system to produce long, aligned fibers. The electric field originates radially from the charged spinneret, directed towards the collector electrodes. Near the electrodes, the electric field lines bend in the horizontal direction, perpendicular to the electrodes. It has been demonstrated that the relative magnitude of this horizontal component of the field increases with increasing gap width, which favors the fiber alignment across the gap.[16] However, there is a maximum electrode gap width within which the high-degree of fiber alignment can be maintained. Above this maximum width, the degree of fiber alignment decreases due to reduced electric field strength that aligns charged fibers. As shown in Fig. 3, a 20 wt% PVDF solution electrospun at 12 kV and 200 rpm spinneret rotating speed produced highly aligned fibers across both a one-inch and a four-inch gap (Fig. 3a and b), but the fibers were not as well aligned on the six-inch gap (Fig. 3c). This was further illustrated by FFT analysis (Fig. 3d). The four-inch electrode gap was thus chosen for further studies described below as it maintains good fiber alignment while producing long fibers.

Polymer concentration

The viscosity of the solution affects the fiber formation, as well as the resultant fiber morphology and diameter. For a given polymer, the solution viscosity depends on the solvent type and polymer concentration. There is a concentration range for each polymer for which continuous nanofibers can be produced. If the polymer concentration is too low, there is insufficient chain entanglement to form continuous fibers; conversely, if the concentration is too high, the resultant high viscosity and surface tension impede solvent evaporation and jet thinning, resulting in large fiber diameters.[24]

In this study, PVDF solutions with polymer concentrations of 20–27.5 wt% were electrospun and evaluated. As shown in Fig. 4, the fiber diameter and non-uniformity increased as the polymer concentration increased; the 20 wt% and 22.5 wt% PVDF solutions yielded more uniform fibers with smaller diameters (Fig. 4a

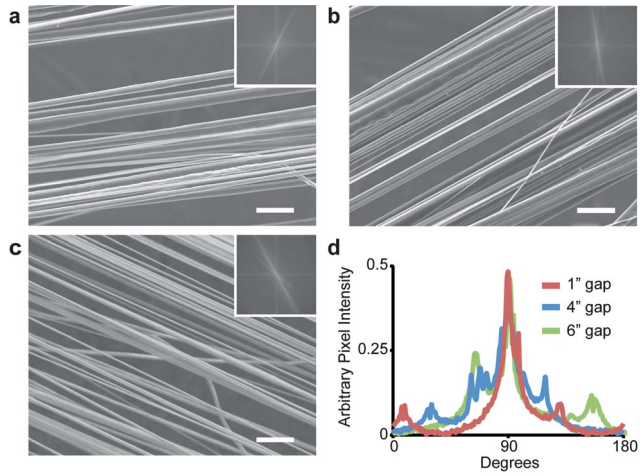

Fig. 3 Influence of the electrode-gap width on the PVDF fiber morphology. SEM images of the PVDF nanofibers from a 20 wt% polymer solution electrospun at 12 kV with a spinneret rotating speed of 200 rpm and retrieved from (a) one-inch, (b) four-inch, and (c) six-inch electrode gaps. The scale bars represent 2 μm. Insets in (a), (b), and (c) are the images from FFT analysis illustrating the degree of alignment. (d) Arbitrary pixel intensity plotted from the radial summation of pixel intensity from the FFT analysis.

and b) than 25 wt% and 27.5 wt% solutions (Fig. 4c and d). For applications where the smallest diameters (thus the greatest surface area-to-volume ratio) are preferred, the optimal PVDF concentration range was 20–22.5 wt% for a spinneret rotating speed of 225 rpm. With the operating parameters chosen from the above investigations, we were able to produce highly aligned PVDF nanofibers with a 20 wt% PVDF solution (Fig. 5).

Using the same methodology shown above, well aligned nanofibers of other polymeric materials can be readily produced with our CE system (see ESI†).

An illustrative application of aligned nanofibers in piezoelectricity

To demonstrate the significance of fiber alignment in practical application, we examined the piezoelectric properties of PVDF fibers. In a traditional piezoelectric application of PVDF, the

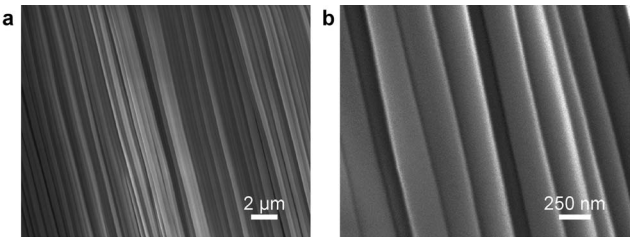

Fig. 5 Highly aligned PVDF fibers produced by the CE system with a 20 wt% polymer solution at 15 kV and 225 rpm.

piezoelectric effect is strongly dependent on the crystalline phase and content (α, β, γ, δ), and PVDF materials can be mechanically or thermally manipulated to induce crystalline changes. Electrospinning has been shown to induce poling of PVDF along the fiber length due to the strong electrical field and mechanical fiber stretching during the electrospinning process.[25] The aligned fibers have been particularly favored for better piezoelectric response.[26] Thus, highly aligned PVDF fibers prepared from our CE system were expected to produce significant piezoelectric responses compared to those prepared by traditional electrospinning methods.

Aligned PVDF fibers were prepared across three-inch electrode gaps at an applied voltage of 15 kV and a spinneret rotating speed of 200 rpm from a 20 wt% PVDF solution with 3 wt% tetrabutyl ammonium chloride (TBAC). For comparison, randomly oriented fibers as well as aligned fibers produced by the parallel electrodes (spinneret rotational speed = 0) were also prepared. All fiber samples were 25 mm long with a cross-sectional area of 0.76 mm^2. The samples were embedded in PDMS, connected *via* electrodes to a voltage-output analyzer and clamped onto a nanomechanical tester that could produce controlled strain rates (Fig. 6a). A common method to measure the piezoelectric response of nanofibers is through a mechanical bending test.[25,27,28] In this study, the fiber/PDMS specimen was deflected in a cantilever motion at one end, which caused a bending strain across the cross-section of the sample and produced a measurable output voltage. The aligned fibers shown in Fig. 5b produced an output voltage of ~3.04 mV at a strain of 0.10 compared to the only 0.059 mV for the randomly oriented fibers. Though the individual PVDF fibers in the randomly

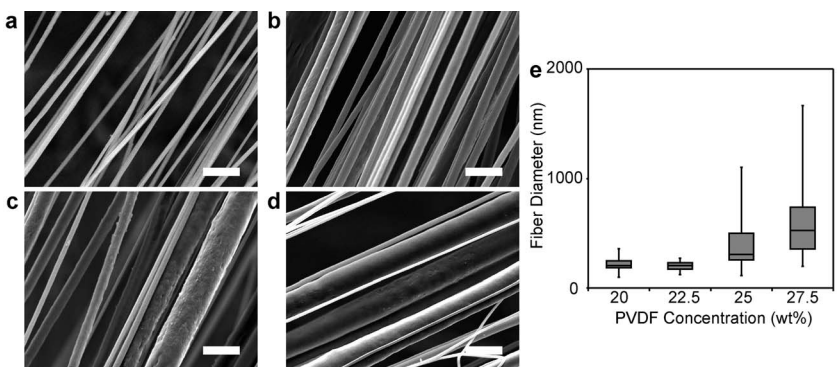

Fig. 4 Influence of the polymer concentration on the morphology of electrospun PVDF fibers. SEM images of fibers produced from (a) 20, (b) 22.5, (c) 25, and (d) 27.5 wt% PVDF in DMF–acetone. The scale bars represent 2 μm. The PVDF solutions were electrospun at 12 kV and 200 rpm, and the fibers were collected from a four-inch electrode gap. (e) Size distribution of electrospun PVDF nanofibers as a function of polymer concentration. The error bars indicate the largest and smallest fiber diameters measured from a dataset of 50 fibers.

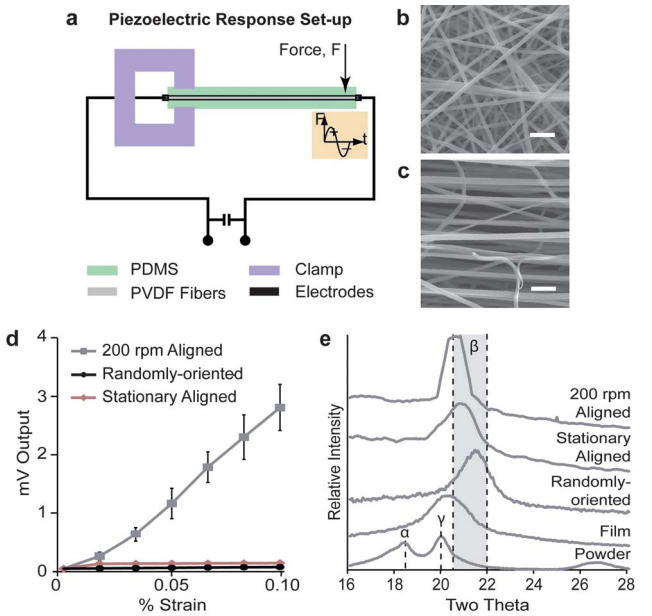

Fig. 6 Piezoelectric effect of PVDF nanofibers. (a) Schematic of the system employed to test the piezoelectric effect of PVDF nanofibers. Aligned nanofibers electrospun at 200 rpm, (b) randomly oriented fibers and (c) stationary spinneret-spun (parallel-electrode) fibers, all 25 mm in length were cast in PDMS, connected to electrodes, fixed *via* a clamp at one end and deflected at the opposite cantilever end. (d) The measured piezoelectric voltage output of fibers produced by the various fibrous systems ($n = 3$ per fibrous system). (e) XRD analysis of the PVDF with designated α-, β-, and γ-phases peak locations.

oriented specimen were likely poled, the randomly oriented poling directions in the membrane's bulk macrostructure (Fig. 6b) resulted in a negligible collective.

Importantly, the partially aligned (Fig. 6c) fibers produced by stationary dispersion (0 rpm, *i.e.* the parallel electrode method) representing the traditional parallel-electrode method produced 0.11 mV voltage outputs. The introduction of a centrifugal dispersion at 200 rpm enhances piezoelectric response by ~27 fold (Fig. 6d) through fiber alignment and molecular poling alignment, demonstrating the potential of the CE technique to produce highly aligned, functional materials for a variety of applications.

XRD analysis was performed to characterize the changes in crystalline phases, which correlate with the piezoelectricity of PVDF, by the introduction of the centrifugal dispersion force *via* the CE system. As shown in Fig. 6e, the original, as-received powder form of the PVDF material exhibited peaks at 18.5° and 20.3° which are associated with the α-[29] and γ-phases of PVDF.[30] In the preparation of the electrospinning solution, PVDF and TBAC were dissolved in a DMF–acetone solvent and refluxed at 80 °C. To demonstrate the effect of the solvent and refluxing on the piezoelectric properties, a film sample was characterized with a single, diffuse γ-phase peak, which corroborates previous results of PVDF in DMF–acetone solution crystalline phases.[31] With the introduction of the electrospinning force, β-phase peaks appear at 20–22°, as shown by the randomly oriented fiber spectra, stationary aligned and centrifugally aligned fibers. The high voltage applied to the electrospinning solution changes the molecular conformation of PVDF and the stretching of the polymer jets results in initial mechanical stretching, which causes nucleation of the β-phase. As all of the electrospun fibers, regardless of dispersion or collection methods, were composed of only the β-phase, there was no significant impact of the centrifugal dispersion on the polymorphism of PVDF. However, as the proposed CE system produced more highly aligned nanofibers than the traditional parallel-electrode method, the resultant PVDF nanofiber responses were enhanced due to the macroscopic anisotropy of the fibers which coincided with the β-phase polarity.

Conclusions

Well-aligned nano-architectures are required in many engineering and biomedical applications to develop sophisticated electrical, chemical or biological devices. Several approaches have been used to modify the collectors of electrospinning systems in order to produce aligned nanofibers. A conventional parallel-electrode electrospinning system can produce nanofibers with a high degree of alignment, but only over a small area. A centrifugal dispersion system, on the other hand, can produce nanofibers over a large area, but the degree of nanofiber alignment is limited. This study presents a new approach to the electrospinning and demonstrates the fabrication of highly aligned and uniform nanofibers over a large area (with fiber length up to several inches). It should be noted that here we only illustrated the basic principle and methodology of the CE system setup and demonstrated how the nanofibrous structure can be modulated by a few key system parameters, and in no way exhausted all the variables that may play a significant role. Other important parameters include the distance between the spinneret and collector, applied voltage, and solution-feeding rate. Also important is the interplay of these variables. The piezoelectric effect of the highly aligned PVDF fibers produced by the CE method demonstrated their potential broad application. Even for a given polymer, different applications require different material properties and thus different system setups. Fortunately, our CE system provides the flexibility to easily adjust the key parameters. For instance, the eight collector gaps between the grounded electrodes in our system can be set to different widths so that the effect of the electrode gap width on the fiber production and properties can be revealed by a single run.

Acknowledgements

This work was supported in part by Kyocera Professor Endowment. The authors would like to thank Vincent Casmirri and Coleen Caputo of Arkema Corporation for supplying the polyvinylidene fluoride and polyvinylidene fluoride tetrafluoroethylene chemicals and Tanner Edmondson for fabrication and assembly assistance.

References

1 F. Gu, L. Zhang, X. Yin and L. Tong, *Nano Lett.*, 2008, **8**, 2757–2761.
2 V. Thavasi, G. Singh and S. Ramakrishna, *Energy Environ. Sci.*, 2008, **1**, 205–221.
3 A. Arinstein, M. Burman, O. Gendelman and E. Zussman, *Nat. Nanotechnol.*, 2007, **2**, 59–62.
4 S. Mitragotri and J. Lahann, *Nat. Mater.*, 2009, **8**, 15–23.

5 N. Nerurkar, B. Baker, S. Sen, E. Wible, D. Elliott and R. Mauck, *Nat. Mater.*, 2009, **8**, 986–992.
6 J. Xie, M. R. MacEwan, X. Li, S. E. Sakiyama-Elbert and Y. Xia, *ACS Nano*, 2009, **3**, 1151–1159.
7 C. Wang, C. Kuo, H. Chen and W. Chen, *Nanotechnology*, 2009, **20**, 375604.
8 T. Tamura and H. Kawakami, *Nano Lett.*, 2010, **10**, 1324–1328.
9 N. Bhardwaj and S. Kundu, *Biotechnol. Adv.*, 2010, **28**, 325–347.
10 J. A. Matthews, G. E. Wnek, D. G. Simpson and G. L. Bowlin, *Biomacromolecules*, 2002, **3**, 232–238.
11 A. Theron, E. Zussman and A. Yarin, *Nanotechnology*, 2001, **12**, 384–390.
12 A. Baji, Y. Mai, S. Wong, M. Abtahi and P. Chen, *Compos. Sci. Technol.*, 2010, **70**, 703–718.
13 W. Teo and S. Ramakrishna, *Nanotechnology*, 2006, **17**, 89–106.
14 D. Li, Y. L. Wang and Y. N. Xia, *Nano Lett.*, 2003, **3**, 1167–1171.
15 V. P. Secasanu, C. K. Giardina and Y. Wang, *Biotechnol. Prog.*, 2009, **25**, 1169–1175.
16 L. Liu and Y. Dzenis, *Nanotechnology*, 2008, **19**, 355307.
17 M. Badrossamay, H. Mcllwee, J. Goss and K. Parker, *Nano Lett.*, 2010, 5456–5464.
18 F. Dabirian, S. Sarkeshik and A. Kianiha, *Curr. Nanosci.*, 2009, **5**, 318–323.
19 W. A. Yee, M. Kotaki, Y. Liu and X. Lu, *Polymer*, 2007, **48**, 512–521.
20 B. O'Connell, Oval Prolife Plot, http://rsbweb.nih.gov/ij/plugins/oval-profile.html.
21 D. Edmondson, N. Bhattarai, S. Jana, A. Kim and M. Zhang, *Appl. Phys. Lett.*, 2009, **94**, 103101.
22 G. Rutledge and S. Fridrikh, *Adv. Drug Delivery Rev.*, 2007, **59**, 1384–1391.
23 D. Reneker, A. Yarin, E. Zussman and H. Xu, *Adv. Appl. Mech.*, 2007, **41**, 43–195.
24 T. Sill and H. von Recum, *Biomaterials*, 2008, **29**, 1989–2006.
25 C. Chang, V. Tran, J. Wang, Y. Fuh and L. Lin, *Nano Lett.*, 2010, **10**, 726–731.
26 J. Zheng, A. He, J. Li and C. C. Han, *Macromol. Rapid Commun.*, 2007, **28**, 2159–2162.
27 X. Chen, S. Xu, N. Yao and Y. Shi, *Nano Lett.*, 2010, **10**, 2133–2137.
28 S.-H. Lee, C. Tekmen and W. M. Sigmund, *Mater. Sci. Eng., A*, 2005, **398**, 77–81.
29 D. M. Esterly and B. J. Love, *J. Polym. Sci., Part B: Polym. Phys.*, 2004, **42**, 91–97.
30 Y. Takahashi and H. Tadokoro, *Macromolecules*, 1980, **13**, 1317–1318.
31 M. Benz, W. B. Euler and O. J. Gregory, *Macromolecules*, 2002, **35**, 2682–2688.